Identification of novel chemical compounds targeting filovirus VP40-mediated particle production

Shuzo Urata[1,2*], Olaposi Idowu Omotuyi[3], Ayako Izumisawa[2], Takeshi Ishikawa[4], Satoshi Mizuta[5], Yasuteru Sakurai[1,2], Tatsuaki Mizutani[5], Hiroshi Ueda[3], Yoshimasa Tanaka[6], Jiro Yasuda[1,2,4*]

[1]Department of Emerging Infectious Diseases, Institute of Tropical Medicine (NEKKEN), Nagasaki University, 1-12-4 Sakamoto, Nagasaki, 852-8523, Japan

[2]National Research Center for the Control and Prevention of Infectious Diseases (CCPID), Nagasaki University, 1-12-4 Sakamoto, Nagasaki, 852-8523, Japan

[3]Department of Pharmacology and Therapeutic Innovation, Graduate School of Biomedical Sciences, Nagasaki University, 1-14 Bunkyo-machi, Nagasaki, 852-8521, Japan

[4]Graduate School of Biomedical Sciences and Program for Nurturing Global Leaders in Tropical and Emerging Communicable Diseases, Nagasaki University, 1-12-4 Sakamoto, Nagasaki, 852-8523, Japan

[5]Center for Bioinformatics and Molecular Medicine, Graduate School of Biomedical Sciences, Nagasaki University, 1-12-4 Sakamoto, Nagasaki, 852-8523, Japan

[6]Center for Medical Innovation Nagasaki University, 1-7-1 Sakamoto, Nagasaki, 852-8588, Japan

*Corresponding author

SU: shuzourata@nagasaki-u.ac.jp

JY: j-yasuda@nagasaki-u.ac.jp

Current address:

O.I.O.: Institute for Drug Research and Development, S.E. Bogoro Center, Afe Babalola University, Ado-Ekiti, Nigeria

TI: Department of Chemistry, Biotechnology, and Chemical Engineering, Graduate School of Science and Engineering, Kagoshima University, Japan

T.M.: Laboratory of Cell Regulation Institute for Frontier Life and Medical Sciences, Kyoto University, Japan

H.U.: Laboratory for the Study of Pain, Research Institute for Production Development, Japan

Abstract

The central role of Ebola virus (EBOV) VP40 in nascent virion assembly and budding from infected host cells makes it an important therapeutic target. The mechanism of dimerization, following oligomerization of VP40 leading to the production of virus-like particles (VLP) has never been investigated for the development of therapeutic candidates against Ebola disease. Molecular dynamics-based computational screening targeted VP40 dimer with 40,000,000 compounds selected 374 compounds. A novel *in vitro* screening assay selected two compounds, NUSU#1 and NUSU#2. Conventional VLP assays consistently showed that both compounds inhibited EBOV VP40-mediated VLP production. Intriguingly, NUSU#1 inhibited the VP40-mediated VLP production in other ebolavirus species and the Marburg virus, but did not inhibit Lassa virus Z-mediated VLP production. These results strongly suggested that the selected compounds are potential lead drug candidates against Filovirus disease via disruption of VP40-mediated particle production.

Introduction

The family *Filoviridae* contains the genera *Ebolavirus*, *Marburgvirus*, *Dianlovirus*, *Striavirus,* and *Thamnovirus,* and the proposed genus *Cuevavirus* [1]. There are six known ebolavirus species: *Zaire ebolavirus*, *Sudan ebolavirus*, *Bundibugyo ebolavirus*, *Tai Forest ebolavirus*, *Reston ebolavirus,* and a putative *Bombali ebolavirus*. Ebola virus (EBOV, species; *Zaire ebolavirus*) causes severe hemorrhagic fever, with a mortality rate of up to 90 % (World Health Organization (WHO): https://www.who.int/news-room/fact-sheets/detail/ebola-virus-disease). Currently, two EBOV vaccines were approved [2]; however, there have been no approved anti-EBOV small molecule therapeutics yet. Recent experimental laboratory infections of mammals and the molecular-biological characterization of distinct filoviruses

indicated the difference in clinical phenotypes and detailed mechanisms of replication in the cells among the Filoviruses [3]. It is thus imperative to develop novel therapy against other filoviruses, not only against EBOV.

Of the seven structural proteins encoded by the EBOV genome, VP40 is known as the main matrix protein that facilitates virion production [4]. The expression of VP40 alone in host cells produces virus-like particles (VLP) [4, 5]. It is also known that VP40 negatively regulate the viral genome replication [6]. Considering the multiple roles of VP40 in the viral life cycle, VP40 could be one of an ideal drug target to combat the Ebola virus disease (EVD). EBOV VP40 is composed of 326 amino acids, and several domains and motifs have been reported to maintain VP40 function during the viral life cycle. The late domain in VP40 is a known domain involved in efficient particle production [7, 8], although it is reported not to be essential [9], through interactions with specific host factors [10], including Tsg101 [11], E3 ligases [12-15], and/or ALIX [16]. Determination of the crystal structure of EBOV VP40 revealed the importance of residues 52–65 and 108–117 [17], as well as T112 and L117 [17], for VP40-VP40 dimerization. This dimerization and subsequent oligomerization processes are important for the assembly and production of VLP [17, 18]. Therefore, inhibiting the function of VP40 on the assembly and budding processes could suppress the nascent virion production.

In this study, *in silico* screening was performed to select compounds from a chemical library consisting of a large number of compounds that may interfere with the EBOV VP40 dimer formation and subsequent VLP production. To evaluate the compounds ranked from the virtual screening, a novel *in vitro* screening method, using a plasmid in which nano-luciferase (Nluc) was tagged with EBOV VP40 at its N-terminus, was established. With this method and a conventional VLP assay, two chemical compounds were shown to inhibit the VP40-

mediated VLP production of EBOV. Of note, the identified compounds also inhibited the VP40-mediated VLP production of other ebolaviruses and Marburg virus (MARV), but not the Lassa virus (LASV; *Arenaviridae*) Z-mediated VLP production. This study is the first to identify novel chemical compounds that exhibited reduction of filoviruses', five species of ebolavirus and MARV, VP40-mediated VLP production. These findings would facilitate the development of novel chemical compounds that target the release of virion production and could be applied in the clinic to treat Filovirus disease (FVD).

Materials and Methods

High-throughput virtual screening. The starting protein structure for molecular docking was the butterfly shaped EBOV VP40 dimer crystallized in a previous study [17]. The compactness of the dimer interface makes pocket selection improbable for molecular docking. To overcome this challenge, the dimer was subjected to 50 ns unrestrained molecular dynamics simulation, following our previously reported protocols [19] and the generated conformations were analyzed using the VMD Vol-Map plugin. VolMap generates volumetric maps of water molecules around the protein [20], where the region within the interface of the two chains with the highest water density was selected as the putative binding pocket for drug target and virtual screening. The ligands for docking were ~40,000,000 unique conformations generated from drug-like compounds (Tokyo University Chemical Database) developed by the University of Tokyo. For all ligands, the MMFF94x force field was used for atom parametrization. Using the molecular operating environment (MOE)-DOCK suite, each conformation was docked into the pre-selected pocket of the VP40 dimer and scored using the affinity-dG algorithm [21] built in MOE-DOCK. Compounds were selected on the basis of dG (< −10.0 *kcal/mol*) ranking, and then filtered down to 374 by excluding compounds with molecular weights > 500 (Fig. 1A).

Cell, plasmids, reagents. The 293T cells were grown in Dulbecco's modified Eagle's medium (Invitrogen) containing 10 % fetal bovine serum (FBS), 100 IU/ml penicillin and 100 μg/mL streptomycin. The pC-FLAG-EBOV VP40, which expresses VP40 with an N-terminal FLAG tag, has been described previously [22]. To construct FLAG-tag expression plasmids for the other EBOV VP40, primer sets were used to amplify the VP40 gene (Supplement Table 1). All products were amplified using polymerase chain reaction (PCR) with the primer 5′- TAAGGACGACGACGACAAAGCAGCC -3′ (forward) and each reverse primer

(Supplement Table 1). The PCR products were further amplified using 5′-CGGAATTCATGGATTATAAGGACGACGACG -3′ and each reverse primer, and digested with EcoRI to insert into the pCAGGS plasmid using Ligation Kit (6023, Takara Bio Inc., Shiga, Japan) according to the manufacturer's instructions. The pCLV-Z-FLAG [23], pMV-VP40 (WT) [24], and mCherry-Lact2 [22] have been described previously. To obtain the pC-Nluc-EBOV VP40 plasmid, the plasmids pNL1.1 (Promega, Madison, WI) and pC-FLAG-EBOV were used as templates for *Nluc* and EBOV VP40, respectively. The *Nluc* and EBOV VP40 were amplified with the primer sets listed in Supplement Table 1 using GXL polymerase (R050A, Takara Bio Inc.). Both PCR fragments were annealed and elongated using KOD plus enzyme (KOD-201, Toyobo, Osaka, Japan) to obtain Nluc-EBOV VP40. The pCAGGS plasmid was digested with EcoRI and ligated with Nluc-EBOV VP40 using the In-fusion HD cloning kit (Z9648N, Takara Bio Inc.). To construct the pC-Nluc EBOV VP40 T112R and pC-Nluc EBOV VP40 L117R, KOD Plus Mutagenesis Kit (SMK-101, Toyobo) and primer sets (Supplement Table 1) were used, with pC-Nluc EBOV VP40 as template. Anti-mouse IgG-FITC and anti-FLAG mouse monoclonal antibodies were purchased from Abcam (ab7064, Cambridge, UK) and Sigma-Aldrich (M2, F3165, Burlington, MA), respectively. An anti-Actin mouse monoclonal antibody (AC-15) was purchased from Sigma-Aldrich. Anti-MARV VP40 rabbit polyclonal antibody [24] has been described previously. Antibodies against rabbit IgG and mouse IgG, both of which conjugated with horseradish peroxidase, were purchased from Promega (W401B) and Sigma-Aldrich (A2304), respectively. The compounds NUSU#1 (NS-01455004, E2615177QS) and NUSU#2 (NS-01462904, E2615185QS) were purchased from Vitas-M (Hong King, China).

***In vitro* screening using a Nluc-EBOV VP40.** The 293T cells (1 x 10^4) were seeded on a 96-well plate (167008, Thermo Fisher Scientific, Waltham, MA) and transfected with 0.1 μg

of pC-Nluc-EBOV VP40, pC-Nluc-EBOV VP40 (T112R), or pC-FLAG-EBOV VP40 (L117R) using LT-1 (Mirus, Madison, WI). To examine the effect of the compounds, culture media were replaced with fresh media containing chemical compounds (100 μM) at 6 h post transfection (h p.t.). At 24 h p.t., both culture supernatant and cells were lysed using an 1X Nano-Glo Assay Reagent (prepared with a mixture of 50X Nano-Glo Luciferase Assay Substrate and Nano-Glo Luciferase Assay Buffer) and incubated for more than 10 min at 25 ˚C. Samples were transferred to a black 96-well plate (475523, Thermo Fisher Scientific), and luminescence was measured using a TRISTAR LB941 (BERTHOLD Technologies, Bad Wildbad, Baden Wurttemberg, Germany). The overall procedure was shown in Fig. 1B, which was made with BioRender.com. The culture supernatant/cell ratio was calculated, and treatment of culture supernatant/cell using dimethyl sulfoxide (DMSO; control) was set as 1.0. The Z′-factor was calculated as 1 − [(3 × standard deviation $(SD)_{100\%}$) + (3 × $SD_{0\%}$)]/[Average $(Av)_{100\%}$ − $Av_{0\%}$)].

Cell viability assay. Cell viability of 293T cells after compounds' treatment was assessed using the CellTiter-Glo Luminescent Cell Viability Assay (Promega), which determines the number of viable cells in a culture based on ATP levels. 293T cells (2×10^4 cells/well) were seeded in 96 well plate to form a monolayer. One day post cell seeding, the cells were treated with 100, 200, 250, or 500 μM of NUSU#1, NUSU#2, or DMSO as a control. At 24 h post-treatment, the culture supernatant was removed, and CellTiter-Glo reagent was added. Thereafter, the assay was performed according to the manufacturer's recommendations using SpectraMAX iD5 (Molecular Device, San Jose, CA). The viability of DMSO-treated control cells was set to 1.0.

VLP assay. The 293T cells (2.5×10^5) were transfected with 0.1 μg of EBOV or MARV VP40 expression plasmid using LT-1 (3 μl LT-1/μg DNA). At 24 h p.t., the VLP-containing culture

supernatants and cells were collected. After removing the cell debris using centrifugation (1,500 × *g*; 5 min), VLP were collected using ultracentrifugation (345,000 × *g*; 30 min at 4 ℃) through a 20 % sucrose cushion [22, 24, 25]. For LASV Z, the same number of cells was transfected with 0.1 μg of pCLV-Z-FLAG. At 24 h p.t., cell debris were removed using centrifugation (1,500 × *g*; 5 min), and VLP-containing culture supernatants and cells were collected using ultracentrifugation (195,000 × *g*; 30 min at 4 °*C*) [23, 26-28]. Cells and VLP were resuspended in lysis buffer (1 % NP-40, 50 mM Tris-HCl [pH 8.0], 62.5 mM EDTA, and 0.4 % sodium deoxycholate) and phosphate buffered saline (PBS) (−), respectively.

Western blotting (WB). Cell lysates or VLP samples were resolved in 12 % sodium dodecyl sulfate-polyacrylamide electrophoresis (SDS-PAGE) gel for VP40 and Actin, and in 15 % SDS-PAGE gel for LASV Z, followed by WB using the indicated antibodies. ECL prime (GE Healthcare, Chicago, IL) and LAS3000 (GE Healthcare) were used to detect the proteins.

Immunofluorescence assay. The 293T cells were transfected with 0.1 μg of pC-FLAG-EBOV VP40 with the mCherry-Lact2 plasmid onto a Millicell EZ slide (5 × 10^4 cells/well; PEZGS0816, Merck Millipore, Burlington, MA). At 6 h p.t., the medium was replaced with fresh media containing DMSO or compounds (200 μM). Cells were fixed with 4 % paraformaldehyde at 24 h p.t. and permeabilized using 0.3 % Triton X-100™ in PBS containing 3 % bovine serum albumin and 10 % FBS for 1 h, and then stained using an anti-FLAG antibody for 2 h at 25 ˚C, followed by anti-mouse IgG-FITC. The samples were examined using fluorescence microscopy (BZ-X710, KEYENCE, Osaka, Japan), and 4′,6-diamidino-2-phenylindole (DAPI) was used to stain nuclei. The number of VP40 and phosphatidylserine (PS) co-localized cells were counted and plotted from 50 randomly selected VP40-PS co-expressing cells.

Results

Evaluation of Nluc-EBOV VP40 as a second screening method. Despite narrowing down the candidate compounds to 374 compounds as described in the Materials and Methods section and shown in Fig. 1A, we aimed to develop a screening system that could be used in *in vitro* assays. To avoid an interruption of the particle production due to the large size of the tagged protein, the 513-nucleotide (171 amino acids) small reporter gene, *Nluc*, was tagged at the N-terminus of the EBOV VP40 gene to express Nluc-EBOV VP40 in the cell. To evaluate if this system works for screening, the 293T cells were seeded in 48 wells of a 96-well plate, and transfection was performed using pC-Nluc-EBOV VP40. Eight wells on both sides of the plate were mock-transfected using an empty plasmid (pCAGGS). Either culture supernatant or cells were mixed with the 1X Nano-Glo Assay Reagent, and the signal was measured as described in the Materials and Methods (Fig. 1B). As shown in Fig. 1C, the signals from the culture supernatant with the pC-Nluc-EBOV VP40 transfection exhibited 4-logs higher signal than the transfection with the pCAGGS. The Z′-factor was calculated as 0.57 (Fig. 1C). Based on this result, the ratio of the signal from culture supernatant divided by the signal from the cell was calculated to evaluate the VLP production. To further confirm that this system reflected VP40-mediated VLP production, threonine (T) at position 112 and leucine (L) at position 117 were mutated to arginine (R). Both mutations disrupt VP40 dimer formation and abrogate VLP production [17]. The relative signal ratio (sup/cell) was significantly reduced in the T112R and L117R mutants compared to that of the VP40 wild-type (Fig. 1D).

Second screening of the compounds using Nluc-EBOV VP40. Using the Nluc-EBOV VP40 assay, a total of 374 compounds selected from *in silico* screening were further

screened to identify compounds that potentially reduce the EBOV VP40-mediated VLP production *in vitro*. After repeating the experiment, treatment with two compounds, NUSU#1 and NUSU#2 (both 100 μM), showed a significant reduction in VP40-mediated VLP production compared to the DMSO control (Fig. 1E). Synta66, which was reported to inhibit EBOV VP40- and LASV Z-mediated VLP production [29], was used as a standard for selecting the hit compounds (Fig. 1E). The effects of NUSU#1 and NUSU#2 on EBOV VP40-T112R and VP40-L117R mediated VLP production were also examined using the Nluc-EBOV VP40 assay. NUSU#1 did not reduce, but rather increase, while NUSU#2 slightly reduced the ratio of Relative Light Units (RLUs) on both EBOV VP40-T112R and VP40-L117R expressed samples compared to the DMSO treatment (Fig. 1F).

Characterization of the two identified compounds. To characterize the inhibitory effect of two hit compounds, NUSU#1 and NUSU#2, different concentrations of the compounds were tested to examine with the Nluc-EBOV VP40 assay (Fig. 2A). As a result, the 50 % inhibitory concentration (IC_{50}) of NUSU#1 and NUSU#2 was calculated as 51.65 μM and 21.78 μM, respectively. The 50% cytotoxic concentration (CC_{50}) was also calculated as 425 μM (NUSU#1) and > 500 μM (NUSU#2) by measuring the cell viabilities on compounds' treated cells between 100 and 500 μM (Fig. 2B). To further confirm their inhibitory effects in VLP production, a conventional VLP assay was performed. The reduction in EBOV VP40-mediated VLP production by the compounds' treatment with NUSU#1 and NUSU#2 was dose-dependent (Fig. 2C). Treatment of NUSU#1 with 200 μM slightly reduced VP40 expression, while Actin expression was not affected.

NUSU#1 and NUSU#2 inhibited VP40-mediated VLP production in four other

ebolavirus species. Since the corresponding amino acids for the dimer formation of VP40 is highly conserved among the ebolavirus species, the activity range of the compounds on the VP40-mediated VLP production was further examined, using Bundibugyo virus, Sudan virus, Tai Forest virus, and Reston virus VP40 (Fig. 3). For the VP40-mediated VLP production in Bundibugyo virus, 100 μM and 200 μM of NUSU#1 and NUSU#2 reduced VLP production (Fig. 3A). For the VP40-mediated VLP production of Sudan virus, 100 μM and 200 μM NUSU#1 also reduced VLP production. In contrast, NUSU#2 did not significantly reduce VLP production (Fig. 3B). Treatment with 100 μM and 200 μM NUSU#1 reduced VP40-mediated VLP production of Tai Forest virus. Similar to Sudan virus, NUSU#2 did not affect Tai Forest virus VP40-mediated VLP production (Fig. 3C). It should be noted that NUSU#1 inhibited Reston virus VP40 expression in cells, which was not observed in the VP40 expression of other ebolavirus species. Due to this observation, relative VLP production was not calculated in NUSU#1-treated samples. NUSU#2 inhibited Reston virus VP40-mediated VLP production (Fig. 3D).

NUSU#1 and NUSU#2 inhibited VP40-mediated VLP production in Marburg virus (MARV), but not Lassa virus (LASV) Z-mediated VLP production. Since NUSU#1 and NUSU#2 reduced the VP40-mediated VLP production of all ebolavirus species tested to a different extent, the effects of the compounds were further examined against the VP40-mediated VLP production of MARV, another filovirus. Treatment with 100 μM and 200 μM NUSU#1 reduced MARV VP40-mediated VLP production. In contrast, NUSU#2 did not significantly reduce MARV VP40-mediated VLP production (Fig. 4A).

EBOV VP40 and MARV VP40 utilize the same host machinery, endosomal sorting complex required for transport (ESCRT), to form a particle and be released from the cell [11, 24]. To

elucidate whether the identified compounds target this host machinery, the effects of NUSU#1 and NUSU#2 on Z-mediated VLP production of LASV, which is also known to utilize the ESCRT machinery to release VLP [26], were examined. As shown in Fig. 4B, neither compound affected the LASV Z-mediated VLP production.

NUSU#1 and NUSU#2 inhibited EBOV VP40 co-localization with phosphatidyl serine (PS). It was reported that the dimer, following hexamer formation of EBOV VP40, is essential for VP40-mediated VLP production [17]. Moreover, PS is recognized by the hexamer form of EBOV VP40 at the plasma membrane (PM) [22, 30]. Therefore, the effects of the selected compounds on the EBOV VP40 recognition of PS at the PM were examined. The mCherry-Lact2 was used to tag the PS [31], as previously we reported [22]. While EBOV VP40 and PS co-localized in the speckle with high frequency (29 cells out of 50 counted cells (58 %)), shown by the white arrow and as observed in our previous study [22], treatment with NUSU#1 (15 cells out of 50 counted cells (30 %)) and NUSU#2 (8 cells out of 50 counted cells (16 %)) significantly reduced the number of co-localized cells (Figs. 5A and 5B).

Discussion

Filovirus disease (FVD), including Ebola virus disease (EVD) and Marburg virus disease (MVD), is caused by filovirus infection [32]. EVD outbreaks have occurred several times. The largest outbreak that started at the end of 2013 was reported to cause 28,652 infections and 11,325 deaths (Centers for Diseases Control (CDC): https://www.cdc.gov/vhf/ebola/history/2014-2016-outbreak/index.html). In the case of the MVD, the number of outbreaks is much more limited, but it has still been reported multiple times in the history (WHO: https://www.who.int/news-room/fact-sheets/detail/marburg-virus-

disease).

Significant efforts have been done to develop prophylaxis and treatment against filovirus infection, and several vaccines and antivirals have been shown to be effective *in vitro* and *in vivo* [33]. In this study, we attempted to identify novel chemical compounds that could interfere with the function of VP40 by inhibiting essential dimer formation [17, 18]. First, we performed with an *in silico* screening to narrow down the candidate compounds from ~40,000,000 virtual three-dimensional conformational libraries. Since large molecular weight (MW) compounds have the potential to inhibit the dimer form non-specifically, compounds larger than 500 MW were excluded in this study. A total of 374 compounds were selected and evaluated for their ability to inhibit VP40-mediated particle release with Nluc tagged EBOV VP40 expression. This newly developed system was suitable for the high-throughput screening as evaluated in Fig. 1C and 1D. Using this *in vitro* screening assay, 374 compounds were narrowed down to two compounds, which exhibited equivalent or higher inhibitory effect on Nluc activity with 100 μM compared to that of 50 μM Synta66 treatment, which was reported to inhibit EBOV VP40-mediated VLP production [29]. The effects of NUSU#1 and NUSU#2 on Nluc-based VLP production were monitored with EBOV VP40 dimerization defect mutants (T112R and L117R). Based on the results (Fig. 1F), it could be assumed that NUSU#1 targeted VP40 dimerization, while NUSU#2 might target another point rather than the dimerization. Since the VLP production from the VP40 dimerization defect mutants was reported to be completely abrogated [17], it is also possible that the very low amount of Nluc in the supernatant from the mutants used here was due to the non-specific release of Nluc from the cell. From measuring both the cell based and culture supernatant based Nluc activities, not only the VLP production but also the cell viability could be monitored. However, one could be careful that the reduction of the Nluc activity from the

cell might be due to the direct effect of the compound to the Nluc and not to the cell viability. Due to this concern, cell viability assay was performed with the identified compounds, NUSU#1 and NUSU#2 (Fig. 2B). Based on the results of the IC_{50} and CC_{50}, the selectivity indices (SI, CC_{50}/IC_{50}) were calculated as 8.22 (NUSU#1) and > 22.9 (NUSU#2), respectively. Although several compounds were ranked as hit compounds, only two compounds exhibited significant reduction of EBOV VP40-mediated VLP production. It is not well known why many of the top ranked compounds from the *in silico* analysis did not show significant reduction of VLP production. One possibility is that the compound binding to the VP40 dimer is not strong enough to antagonize its function and/or could not reach to where VP40 dimer forms. Therefore, the identification of the biology of VP40 dimer formation in the cell and the factors to reach compounds in the VP40 dimer pocket might improve the selection procedure. With the conventional VLP assay, NUSU#1 and NUSU#2 inhibited almost all tested ebolavirus VP40-mediated VLP production, except those in Sudan virus and Tai Forest virus using NUSU#2. In the case of Reston virus, VP40 expression level in cells was reduced upon NUSU#1 treatment; therefore, the relative VLP production was not evaluated. Intriguingly, NUSU#1 inhibited the VP40-mediated VLP production of MARV, which also belongs to *Filoviridae* (Fig. 4A). In contrast, these compounds did not have any effect on the LASV Z-mediated VLP production (Fig. 4B), suggesting that the effect of the two compounds on VLP reduction is limited to *Filoviridae*. Further experiments are required to rule out why both compounds showed different outcomes among *Filoviridae,* even though all ebolaviruses consistently contained T112 and L117. While other amino acids surrounding these two amino acids are also highly conserved, few amino acids are not conserved among the ebolaviruses. These differences might cause slight changes in the VP40 structure, resulting in different outcomes.

Despite the huge effort we exerted to confirm that the compounds identified in our study inhibit EBOV VP40 dimer formation, we could not confirm at this point. Although our initial target was to inhibit the dimer formation of EBOV VP40, we could not exclude the possibility that these compounds target other factors to inhibit the release of filovirus particles. EBOV VP40 recognizes PS, which is exposed at the PM, and precedes particle formation and production. Therefore, we examined whether these compounds inhibited VP40 recognition by PS at the PM [22]. This experiment clearly showed that treatment with both compounds reduced the co-localized cell number of EBOV VP40 and PS (Fig. 5), strongly suggested that the compounds inhibit VP40 transportation to the PM, which might be the result from the disruption of the VP40 oligomerization. In fact, it was reported that dimerization-defective VP40 mutants exhibited a diffuse cytoplasmic localization [34]. However, it is still possible that the identified compounds target the host factor which is involved in the VP40 transportation to the PM and the VLP production. Results from Fig. 1F and Fig. 5 suggested that the target of NUSU#2 might be a host factor which is involved in VP40 transportation to the PM.

Up to now, huge efforts have been put to identify anti-filovirus compounds. In case of targeting VP40-meidated VLP production, small chemical compound, 5539-0062, was reported to inhibit interaction between PTAP motif of EBOV VP40 and Tsg101 with > 90% reduction of VLP production at 100 μM [35]. Likely, the compound 0013 was reported to inhibit Junin virus Z-mediated particle production through interfering the interaction between PTAP motif of Z protein and Tsg101 with the EC_{50} in the nanomolar range [36]. The compound 4 and compound 5 were reported to reduce VLP production 3 to 10 folds by inhibiting PPXY motif of VP40 and Nedd4 with 0.5-1.0 μM [37]. The imatinib and nilotinib, the Abl-family kinase inhibitors, were also reported to inhibit VP40-mediated VLP production through

blocking VP40 phosphorylation [38]. The sangivamycin was reported to inhibit EBOV VP40 mediated VLP production with SI > 2000 (EC_{50}: 0.03 μM, CC_{50}: > 60 μM) [34]. Compared to these reported compounds, NUSU#1 and NUSU#2 exhibited higher EC_{50}. Therefore, it is expected to develop more effective compounds from NUSU#1 or NUSU#2 as leading compounds.

Future studies are needed to identify the exact target of the two compounds, and this study will facilitate the characterization of their detailed mode of action.

Acknowledgements

This study was financially supported by a research grant from the Astellas Foundation for Research on Metabolic Disorders, Kanae Foundation for the Promotion of Medical Sciences, and KAKENHI (Grant-in-Aid for Scientific Research (C), 21K07043) to SU and by the Japan Agency for Medical Research and Development (AMED) to JY (Japanese Initiative for Progress of Research on Infectious Disease for Global Epidemic [J-PRIDE]). This work was (partially) supported by the Platform Project for Supporting in Drug Discovery and Life Science Research from AMED. We are grateful to all the members of the Department of Emerging Infectious Diseases, Institute of Tropical Medicine (NEKKEN), Nagasaki University. We would like to thank Editage (www.editage.com) for English language editing.

Declaration of competing interest

The authors declare no competing financial interests.

Keywords

anti-ebolavirus compound; Ebola virus VP40; viral particle production

Highlights

- *In silico* high-throughput screening of chemical compounds was performed to identify novel anti-Ebola virus compounds targeting the dimer form of Ebola virus VP40.
- A novel *in vitro* screening assay was developed to screen chemical compounds that target Ebola virus particle production.
- Two novel chemical compounds that interfere with ebolavirus particle production were identified.
- One of the identified chemical compounds exhibited anti-pan-filovirus VP40-mediated particle production.

Glossary

EBOV, Ebola virus; Nluc, Nano-luciferase; VLP, virus-like particles; PS, Phosphatidyl-serine

Figure legends

Figure 1. Identification of novel chemical compounds inhibiting Ebola virus (EBOV) VP40-mediated VLP production. (A) Overall scheme of this study to identify compounds that inhibit VP40-mediated VLP production. (B) Schematic representation of the *in vitro* screening assay procedure using Nluc-EBOV VP40. (C) Evaluation of the Nluc-EBOV VP40 assay (in a 96-well plate format) to use for the screening of compounds. Either empty plasmid (pCAGGS) or pC-Nluc EBOV VP40 was transfected in the cells. At 24 h p.t., both culture supernatant (Sup) and cell lysate (Cell) were collected to measure Nluc activities. The Z'-factor was calculated as described in the Materials and Methods. (D) Validation of the Nluc-EBOV VP40 assay using mutants (T112R or L117R), which are known to be abrogated the VLP production [17]. (E) Using Nluc-EBOV VP40 assay, 374 compounds selected from the *in silico* screening were narrowed down to two compounds (NUSU#1 and NUSU#2). These compounds showed less than 50 % of the relative VLP production and more than 80 % cell viability at 100 μM. Synta66 (50 μM) was used as a standard for selecting the active compounds. (F) Evaluation of the NUSU#1 and NUSU#2 on two VP40 mutants (T112R or L117R) mediated VLP production using Nluc-EBOV VP40 assay. The VLP production from DMSO control treatment was set as 1.0. The exact average and SD of relative VLP production compared to DMSO treatment (100 %) were depicted on top of the figure (%).

Figure 2. Evaluation of two identified chemical compounds on EBOV VP40-mediated VLP production. (A) Chemical structures of identified chemical compounds, NUSU#1 and NUSU#2. Using Nluc-EBOV VP40 assay, inhibitory effects of VLP production are plotted with different concentrations of each compound and calculated IC_{50} of each compound is shown. (B) Cell viabilities upon NUSU#1 and NUSU#2 treatment (100, 200, 250, or 500 μM) in 293T

cells. Calculated CC_{50} of each compound is shown. (C) Evaluation of NUSU#1 and NUSU#2 on EBOV VP40-mediated VLP production using conventional VLP assay. The left panel shows the representative result of VLP- and cell-associated VP40 expression upon DMSO control treatment or either 100 μM and 200 μM of NUSU#1 and NUSU#2 using anti-FLAG antibody and cell-associated Actin (control) expression. The right panel shows the average and standard deviation of relative VLP production calculated from independent experiments (n=3). The VLP production from DMSO control treatment was set as 1.0. The exact average and SD of relative VLP production compared to DMSO treatment (100 %) were depicted on top of the figure (%).

Figure 3. Effect of NUSU#1 and NUSU#2 on the VP40-mediated VLP production in Bundibugyo virus, Sudan virus, Tai Forest virus, and Reston virus. Conventional VLP assay was performed to examine the effect of NUSU#1 and NUSU#2 (100 μM and 200 μM, respectively) on VP40-mediated VLP production of (A) Bundibugyo virus, (B) Sudan virus, (C) Tai Forest virus, and (D) Reston virus. The representative result from the WB is shown in the left panel. VLP- and cell-associated VP40 expression was detected using anti-FLAG antibody. Cell-associated Actin expression was also detected. The right panel shows the average and standard deviation of relative VLP production calculated from independent experiments (n=3). The VLP production from the DMSO control treatment was set as 1.0. The VLP production from the DMSO control treatment was set as 1.0. The exact average and SD of relative VLP production compared to the DMSO treatment (100 %) were depicted on top of the figure (%). The treatment with 100 μM and 200 μM NUSU#1 reduced the Reston virus VP40 expression in cells; therefore, the relative VLP production was not shown in the graph (D, right).

Figure 4. Effect of NUSU#1 and NUSU#2 on the VP40-mediated VLP production in Marburg virus (MARV) and Z-mediated VLP production in Lassa virus. (A) Conventional VLP assay was performed to examine the effect of NUSU#1 and NUSU#2 (100 μM and 200 μM, respectively) on (A) MARV VP40- and (B) Lassa virus Z-mediated VLP production. The representative result from the WB is shown in the left panel. VLP- and cell-associated VP40 or Z expression was detected using an anti-FLAG antibody. Cell associated Actin expression was also detected. The right panel shows the average and standard deviation of relative VLP production calculated from independent experiments (n=3). The VLP production from the DMSO control treatment was set as 1.0. The exact average and SD of relative VLP production compared to DMSO treatment (100 %) were depicted on top of the figure (%).

Figure 5. Effect of NUSU#1 and NUSU#2 on the localization of EBOV VP40 and phosphatidyl serine (PS). An immunofluorescence assay was performed to identify the subcellular localization and co-localization with PS of EBOV VP40 upon DMSO control, NUSU#1, and NUSU#2 treatments in 293T cells. The 293T cells were transfected with FLAG-tagged EBOV VP40 expressing plasmids, together with the mCherry-LactC2 plasmid. The LactC2 is known to be a specific sensor for PS. At 6 h p.t., culture media was replaced to fresh media containing DMSO or 200 μM of NUSU#1 and NUSU#2. At 24 h p.t., cells were fixed and stained with an anti-FLAG antibody, followed by an FITC-conjugated secondary antibody. Nuclei were stained with DAPI. Fluorescent microscopy (BZ-X710) was used to observe multiple cells simultaneously (Objective lens, x40, Bar, 20 μm). Captured picture from the right bottom is enlarged below. White arrows indicate co-localization of EBOV VP40 and PS. (B) The VP40 and PS co-localized cells were counted and plotted from 50 randomly

selected VP40-PS co-expressed cells.

References

1. Burk, R., et al., *Neglected filoviruses.* FEMS Microbiol Rev, 2016. **40**(4): p. 494-519.
2. Callaway, E., *'Make Ebola a thing of the past': first vaccine against deadly virus approved.* Nature, 2019. **575**(7783): p. 425-426.
3. Kuhn Jens H., A.G.K., Perry Donna L., *Filoviridae.* Fields Virology, 2021. **1**(seventh edition).
4. Jasenosky, L.D., et al., *Ebola virus VP40-induced particle formation and association with the lipid bilayer.* J Virol, 2001. **75**(11): p. 5205-14.
5. Noda, T., et al., *Ebola virus VP40 drives the formation of virus-like filamentous particles along with GP.* J Virol, 2002. **76**(10): p. 4855-65.
6. Hoenen, T., et al., *Both matrix proteins of Ebola virus contribute to the regulation of viral genome replication and transcription.* Virology, 2010. **403**(1): p. 56-66.
7. Irie, T., J.M. Licata, and R.N. Harty, *Functional characterization of Ebola virus L-domains using VSV recombinants.* Virology, 2005. **336**(2): p. 291-8.
8. Licata, J.M., et al., *Overlapping motifs (PTAP and PPEY) within the Ebola virus VP40 protein function independently as late budding domains: involvement of host proteins TSG101 and VPS-4.* J Virol, 2003. **77**(3): p. 1812-9.
9. Neumann, G., et al., *Ebola virus VP40 late domains are not essential for viral replication in cell culture.* J Virol, 2005. **79**(16): p. 10300-7.
10. Timmins, J., et al., *Ebola virus matrix protein VP40 interaction with human cellular factors Tsg101 and Nedd4.* J Mol Biol, 2003. **326**(2): p. 493-502.
11. Martin-Serrano, J., T. Zang, and P.D. Bieniasz, *HIV-1 and Ebola virus encode small peptide motifs that recruit Tsg101 to sites of particle assembly to facilitate egress.* Nat Med, 2001. **7**(12): p. 1313-9.
12. Harty, R.N., et al., *A PPxY motif within the VP40 protein of Ebola virus interacts physically and functionally with a ubiquitin ligase: implications for filovirus budding.* Proc Natl Acad Sci U S A, 2000. **97**(25): p. 13871-6.
13. Yasuda, J., et al., *Nedd4 regulates egress of Ebola virus-like particles from host cells.* J Virol, 2003. **77**(18): p. 9987-92.
14. Han, Z., et al., *ITCH E3 Ubiquitin Ligase Interacts with Ebola Virus VP40 To Regulate Budding.* J Virol, 2016. **90**(20): p. 9163-71.
15. Martin-Serrano, J., et al., *HECT ubiquitin ligases link viral and cellular PPXY motifs to the vacuolar protein-sorting pathway.* J Cell Biol, 2005. **168**(1): p. 89-101.
16. Han, Z., et al., *ALIX Rescues Budding of a Double PTAP/PPEY L-Domain Deletion Mutant of Ebola VP40: A Role for ALIX in Ebola Virus Egress.* J Infect Dis, 2015. **212 Suppl 2**: p. S138-45.

17. Bornholdt, Z.A., et al., *Structural rearrangement of ebola virus VP40 begets multiple functions in the virus life cycle.* Cell, 2013. **154**(4): p. 763-74.
18. Hoenen, T., et al., *Oligomerization of Ebola virus VP40 is essential for particle morphogenesis and regulation of viral transcription.* J Virol, 2010. **84**(14): p. 7053-63.
19. Omotuyi, O.I. and H. Ueda, *Molecular dynamics study-based mechanism of nefiracetam-induced NMDA receptor potentiation.* Comput Biol Chem, 2015. **55**: p. 14-22.
20. Omotuyi, O.I., J. Nagai, and H. Ueda, *Lys39-Lysophosphatidate Carbonyl Oxygen Interaction Locks LPA1 N-terminal Cap to the Orthosteric Site and partners Arg124 During Receptor Activation.* Sci Rep, 2015. **5**: p. 13343.
21. Omotuyi, O.I., *Methyl-methoxylpyrrolinone and flavinium nucleus binding signatures on falcipain-2 active site.* J Mol Model, 2014. **20**(8): p. 2386.
22. Urata, S., T. Ishikawa, and J. Yasuda, *Roles of YIGL sequence of Ebola virus VP40 on genome replication and particle production.* J Gen Virol, 2019. **100**(7): p. 1099-1111.
23. Urata, S. and J. Yasuda, *Cis- and cell type-dependent trans-requirements for Lassa virus-like particle production.* J Gen Virol, 2015. **96**: p. 1626-1635.
24. Urata, S., et al., *Interaction of Tsg101 with Marburg virus VP40 depends on the PPPY motif, but not the PT/SAP motif as in the case of Ebola virus, and Tsg101 plays a critical role in the budding of Marburg virus-like particles induced by VP40, NP, and GP.* J Virol, 2007. **81**(9): p. 4895-9.
25. Urata, S. and J. Yasuda, *Regulation of Marburg virus (MARV) budding by Nedd4.1: a different WW domain of Nedd4.1 is critical for binding to MARV and Ebola virus VP40.* J Gen Virol, 2010. **91**(Pt 1): p. 228-34.
26. Urata, S., et al., *Cellular factors required for Lassa virus budding.* J Virol, 2006. **80**(8): p. 4191-5.
27. Urata, S., N. Ngo, and J.C. de la Torre, *The PI3K/Akt Pathway Contributes to Arenavirus Budding.* J Virol, 2012. **86**(8): p. 4578-85.
28. Urata, S., et al., *Antiviral activity of a small-molecule inhibitor of arenavirus glycoprotein processing by the cellular site 1 protease.* J Virol, 2011. **85**(2): p. 795-803.
29. Han, Z., et al., *Calcium Regulation of Hemorrhagic Fever Virus Budding: Mechanistic Implications for Host-Oriented Therapeutic Intervention.* PLoS Pathog, 2015. **11**(10): p. e1005220.
30. Adu-Gyamfi, E., et al., *Host Cell Plasma Membrane Phosphatidylserine Regulates the Assembly and Budding of Ebola Virus.* J Virol, 2015. **89**(18): p. 9440-53.

31. Shi, J., et al., *Lactadherin binds selectively to membranes containing phosphatidyl-L-serine and increased curvature.* Biochim Biophys Acta, 2004. **1667**(1): p. 82-90.
32. Kuhn, J.H., et al., *New filovirus disease classification and nomenclature.* Nat Rev Microbiol, 2019. **17**(5): p. 261-263.
33. Hoenen, T., A. Groseth, and H. Feldmann, *Therapeutic strategies to target the Ebola virus life cycle.* Nat Rev Microbiol, 2019. **17**(10): p. 593-606.
34. Bennett, R.P., et al., *A Novel Ebola Virus VP40 Matrix Protein-Based Screening for Identification of Novel Candidate Medical Countermeasures.* Viruses, 2020. **13**(1).
35. Liu, Y., et al., *Bimolecular Complementation to Visualize Filovirus VP40-Host Complexes in Live Mammalian Cells: Toward the Identification of Budding Inhibitors.* Adv Virol, 2011. **2011**.
36. Lu, J., et al., *A host-oriented inhibitor of Junin Argentine hemorrhagic fever virus egress.* J Virol, 2014. **88**(9): p. 4736-43.
37. Han, Z., et al., *Small-molecule probes targeting the viral PPxY-host Nedd4 interface block egress of a broad range of RNA viruses.* J Virol, 2014. **88**(13): p. 7294-306.
38. Garcia, M., et al., *Productive replication of Ebola virus is regulated by the c-Abl1 tyrosine kinase.* Sci Transl Med, 2012. **4**(123): p. 123ra24.

A.

40,000,000 conformation library

↓ *In silico* screening
"MD-based docking assay between VP40 and compound"

374 compounds

↓ Nluc-EBOV VP40 VLP assay
"High-throughput screening for the VLP production"

Hit compounds (NUSU#1 and NUSU#2)

B.

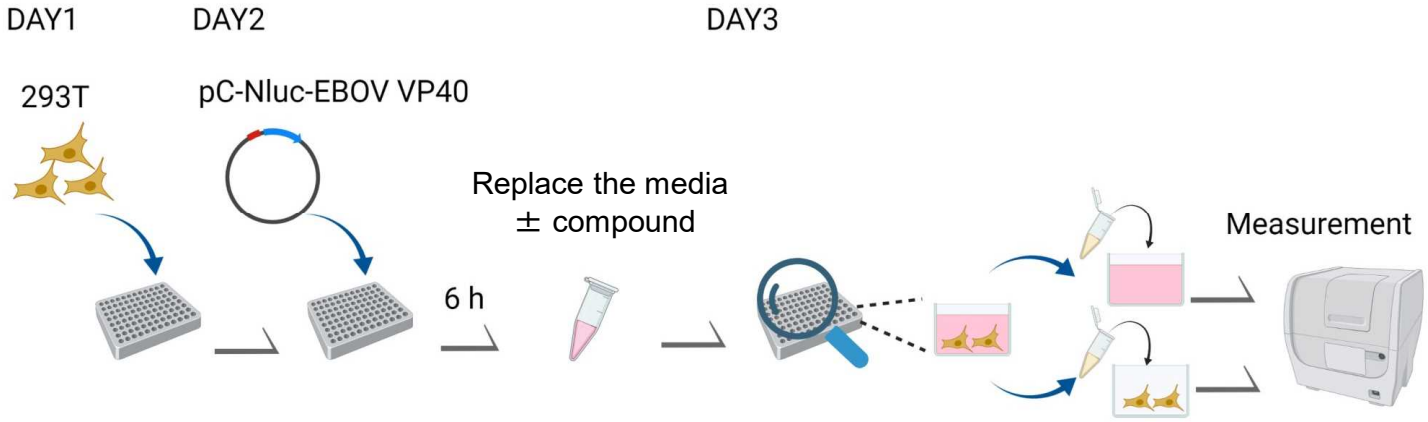

C.

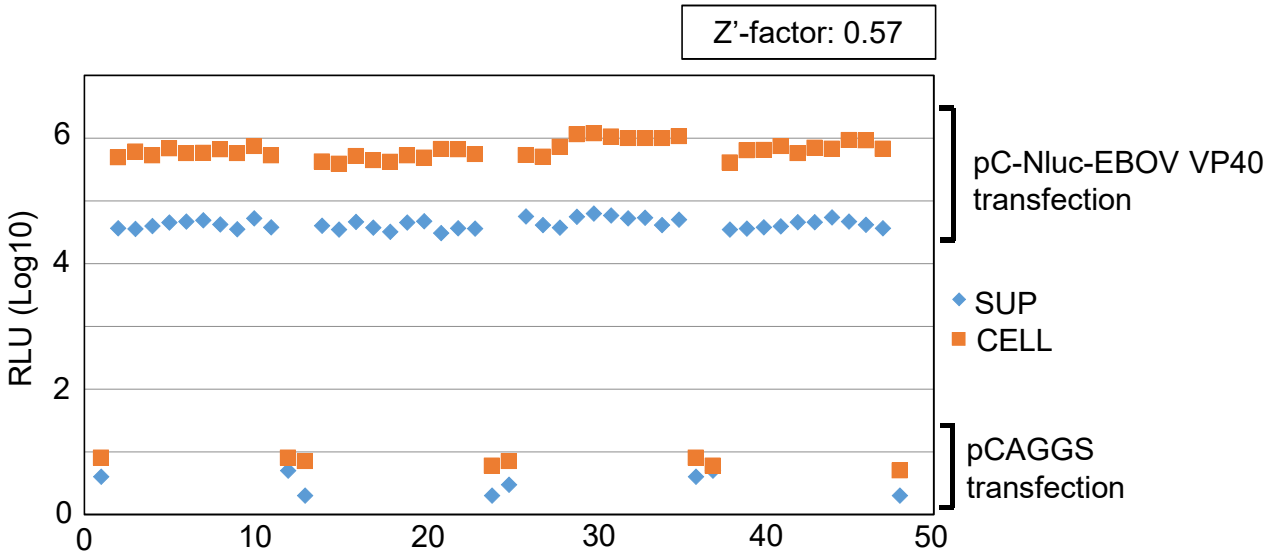

Figure 1A-1C. Urata *et al*.

D.

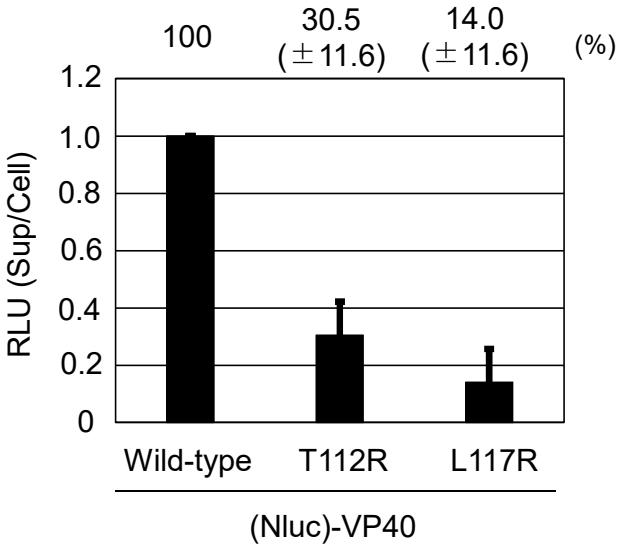

E.

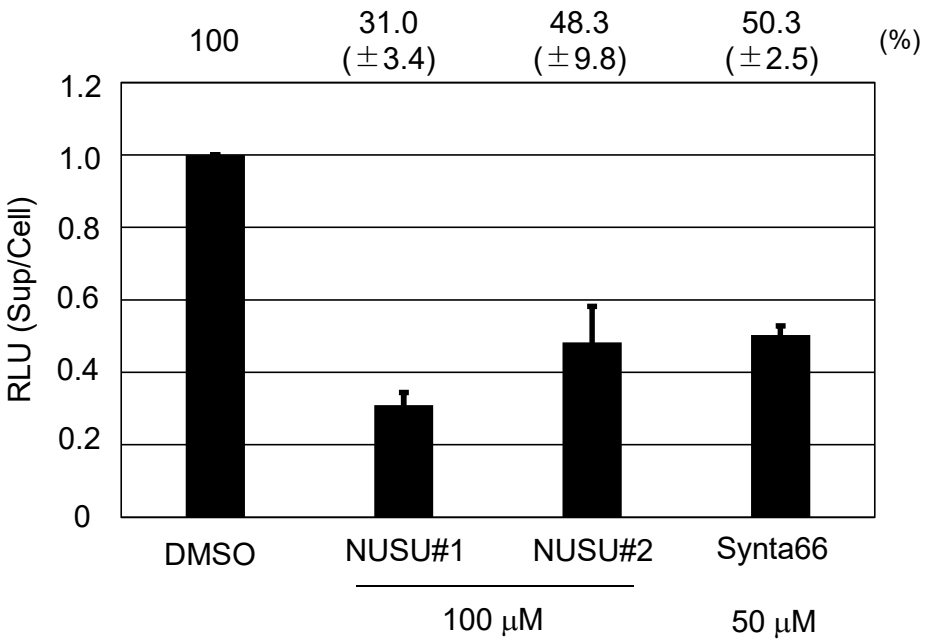

F.

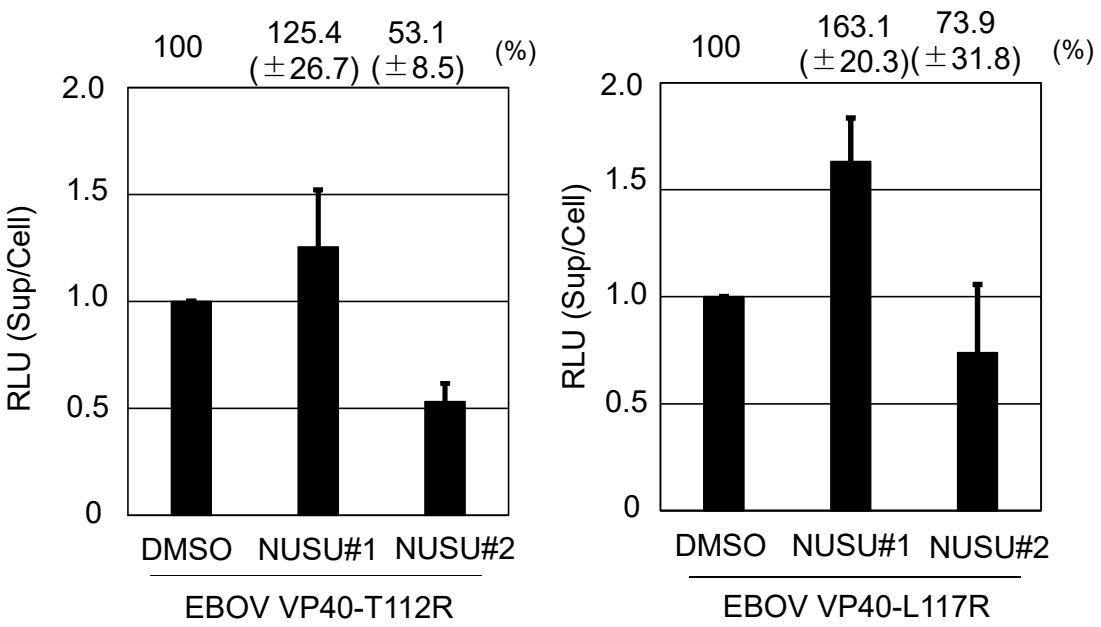

Figure 1D-1F. Urata *et al.*

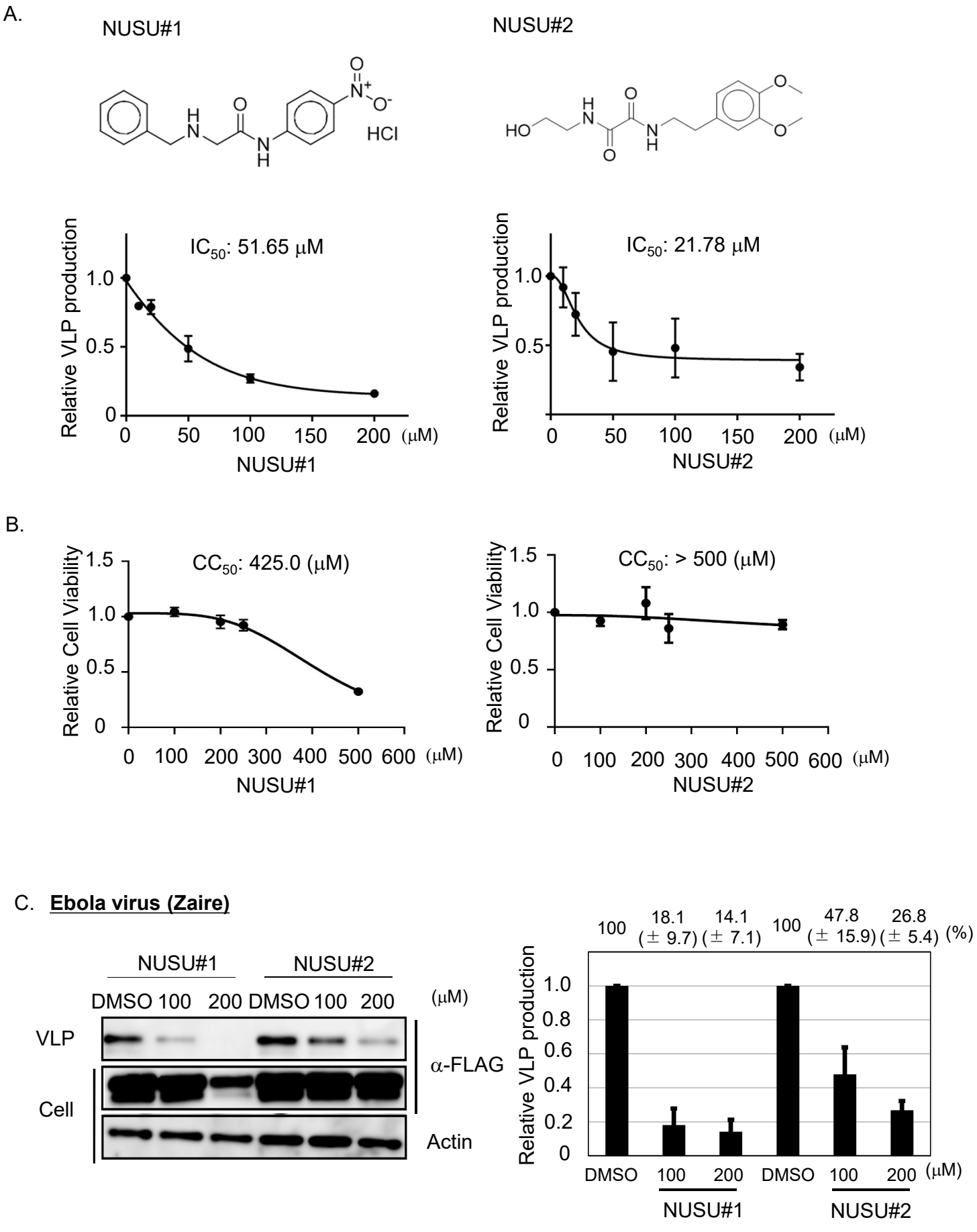

Figure 2. Urata *et al.*

A. **Bundibugyo virus**

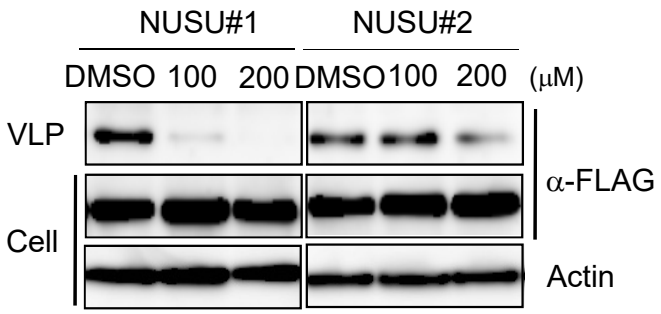

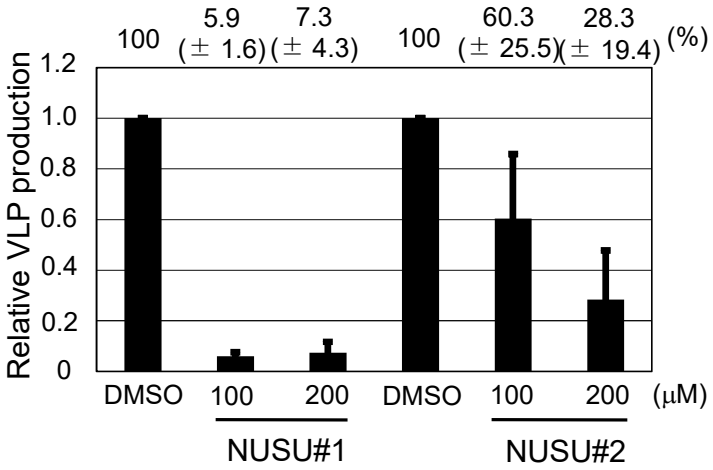

B. **Sudan virus**

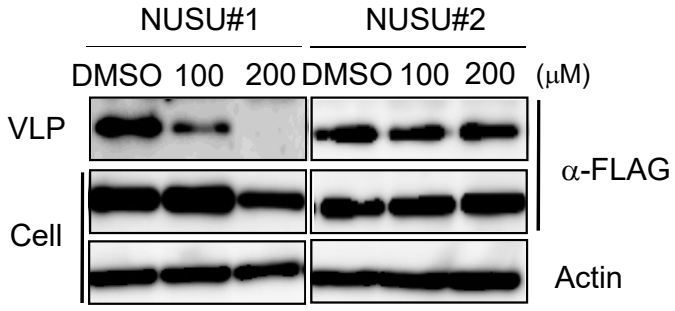

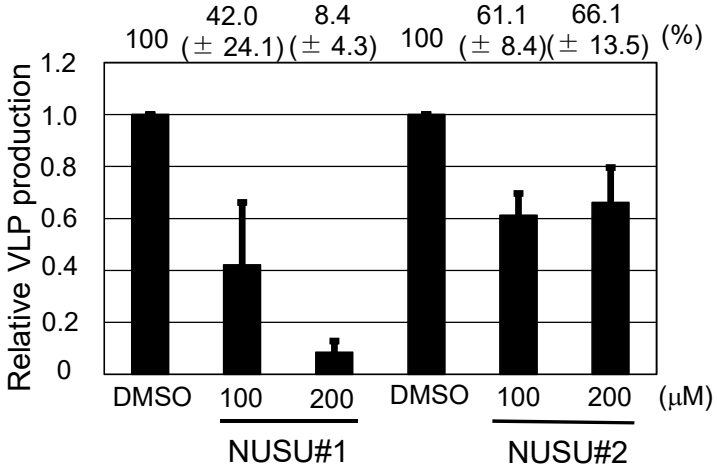

C. **Tai Forest virus**

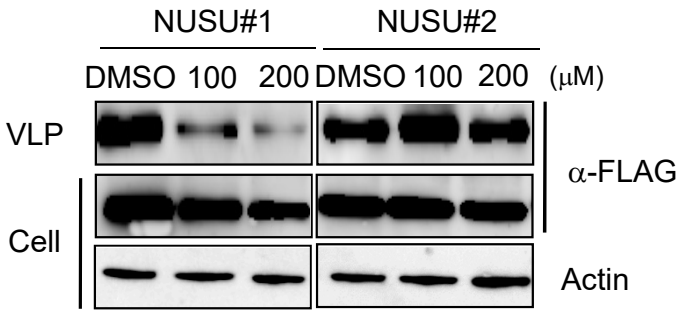

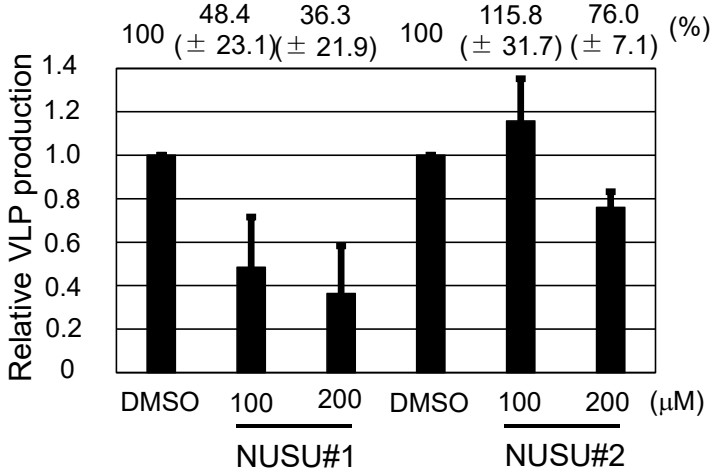

D. **Reston virus**

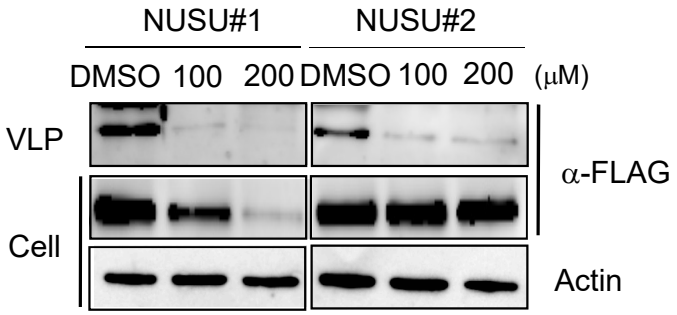

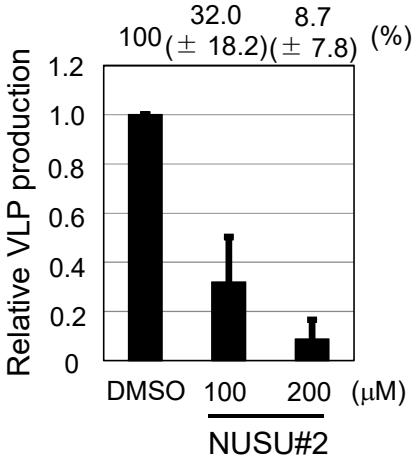

Figure 3. Urata *et al.*

A. **MARV VP40**

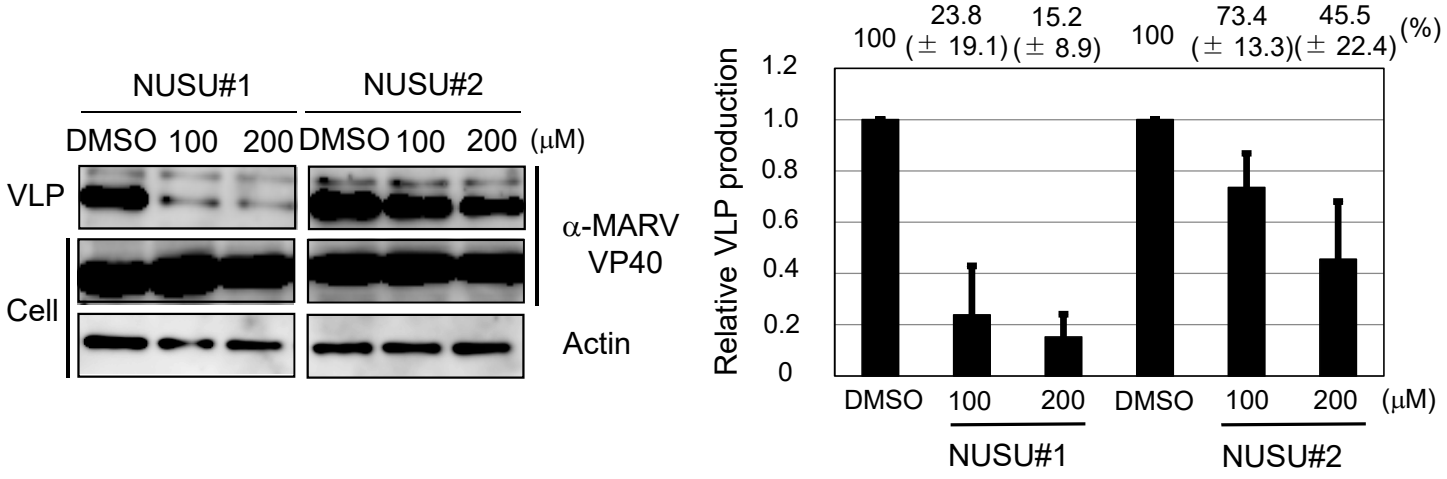

B. **LASV Z**

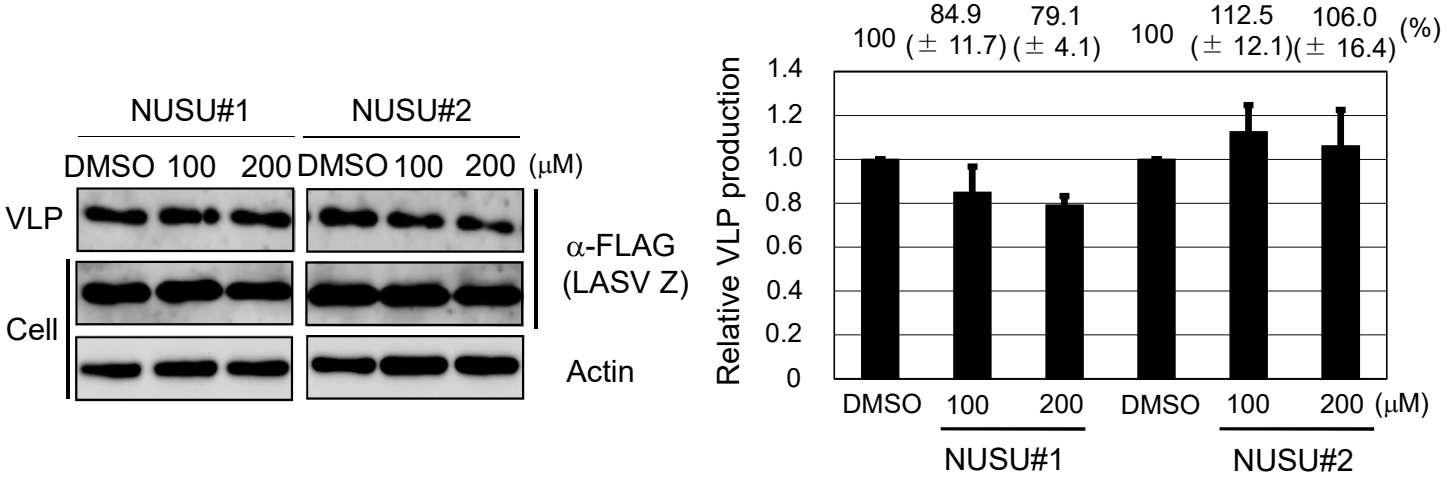

Figure 4 Urata *et al.*

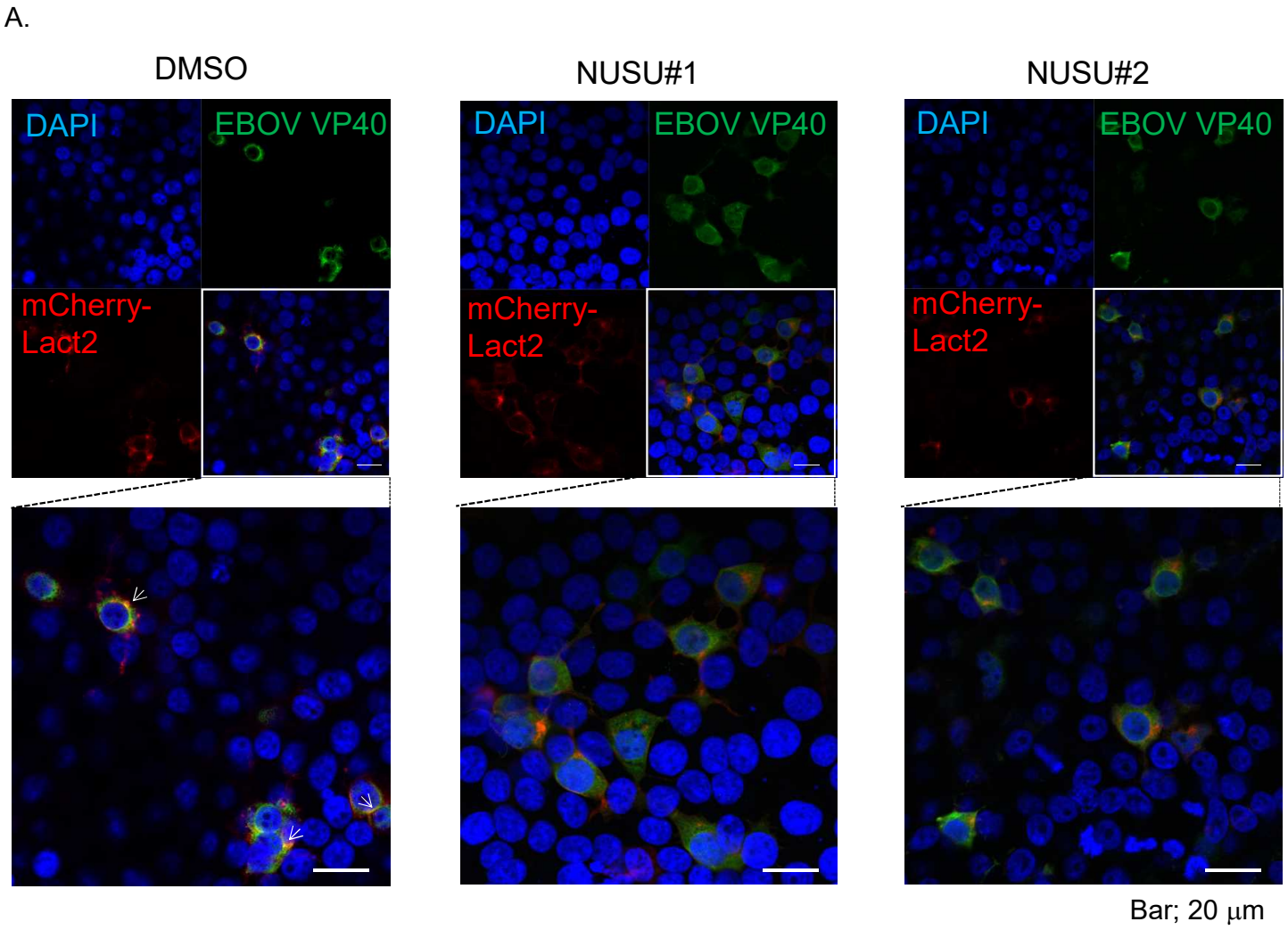

Figure 5. Urata *et al.*

Primer sets for cloning VP40s		
	Forward	Reverse
Sudan virus VP40	5'- CGACAAAGCAGCCAGAAGGGTTACTGTGCC -3'	5'- GCGAATTCTCACTTTTCACTGAGATAAGAG -3'
Reston virus VP40	5'-CGACAAAGCAGCCAGGCGCGGAGTGTTACC -3'	5'- GCGAATTCTTATTGGTAACTATTCTGCTTG -3'
Tai forest virus VP40	5'- CGACAAAGCAGCCAGGAGAATCATCCTACC -3'	5'- GCGAATTCTCATTTTTCATTGACTGGGGG -3'
Bundibugyo virus VP40	5'- CGACAAAGCAGCCAGGAGGGCAATTCTACC -3'	5'- GCGAATTCTCATGCTCATTTCTCGCTGAC -3'
Primer sets for Nluc and VP40 amplification		
	Forward	Reverse
Nluc	5'- TGGCAAAGAATTACCATGGTCTTCACACTC -3'	5'- TATAACCCGCCTTGCTGCCGCCAGAATGCG -3'
EBOV VP40	5'- CGCATTCTGGCGGCAGCAAGGCGGGTTATA -3'	5'- CCTGAGGAGTGAATTTTACTTCTCAATCAC -3'
Primer sets for EBOV VP40 T112R and L117R construction		
T112R	5'- GGGCCGCCATCATGCTTGCTTCATAC -3'	5'- TAGTTGAGTCAAAGCTGTAGGTCTTTTG -3'
L117R	5'- GTGCTTCATACACTATCACCCATTTCGG -3'	5'- GCATGATGGCGGCCGTAGTTGAGTC -3'

Supplement Table 1, primer sets in this study